Universidad Autónoma de Baja California
Chemical Sciences and Engineering Faculty

Thesis title:
Spatial Analysis of Interferograms by Means of the Carré Asynchronous Algorithm

Bachelor's Thesis

by

Eduardo Alejandro del Corral Lira

October 2009

Thesis Director:
Dr. Luis Salas (UNAM) Dr. Esteban Luna (UNAM)
Dr. Adriana Nava Vega (UABC)

Objective

To showcase the three dimensional measurement of an object's surface by means of Carré's asynchronous algorithm using one image. The importance of surface measurement is discussed, as well as the theory behind this algorithm. A review of the fundamental concepts of digital signal processing required is given in an appendix in order to make this information within the reach of a second year bachelor's student. Different evaluation criteria are shown during the analysis, so the results of this thesis can be of use for future development.

Overview

1.1 Surface measurement and its applications

Industry often requires the measurement of surfaces be it for tribology (science and technology of surfaces in contact under relative motion [1]) [2], mechanical inspection [3], design [4], quality control [5]- [6], artificial vision [7]- [8]- [9] or just for obtaining the three-dimensional form of an object [10].

Now at days it is possible to obtain measurements for massive objects as well as fractions of a nanometer, showing the atoms of a surface [1]. Exchanging area of measurement for measurement resolution.

Initially, object profiles were determined manually using the nail (or a coin) and the eye, graphing its surface on paper. Two different approaches emerged, those based on the contact of the nail and those based on visual inspection. Techniques based on contact use a device (generally a stylus) that touches the entire contour of the object to measure [11]. They have the disadvantage of being slow and deteriorating the surface measured. There are also pneumatic techniques, they possess great robustness but offer little detail [3].

Techniques based on the human eye, tend to observe the response of a phenomena such as an acoustic wave, capacitance or some optic property (the last category being the most common and varied) [12]. Optical metrology techniques generally use some form of incident or blocked light on the object. The light source can be focused or not, and use defined wavelength or a determined spectrum. Optical metrology techniques include stereoscopy, holography, confocal microscopy, interferometric techniques and fringe projection [13] [1] [14]. The methods and algorithms studied in this thesis are applied to fringe projection, as well as multiple interferometric techniques. Describing some interferometic techniques and fringe projection in detail, since these techniques share analysis tools all results of this thesis may be applied to both.

1.1.1 Fringe projection

Fringe projection is a non-contact surface measurement technique. A generally monochromatic structured light form is projected on an object, capturing the generated pattern by means of a camera [15] [10], these elements are shown in Figure 1.1.

Depending on the object, multiple projection patterns may be used [10]. However, a commonly employed pattern is sinusoidal fringes, that is that the intensity varies in a sinusoidal manner in one direction and repeats itself in the other. The sine form commonly traverses the columns and repeats itself in all rows, generating vertical fringes as shown in Figure 1.2 being the arrangement employed throughout this thesis. However, horizontal

or rotated fringes may also be used (there are algorithm designed for this setup [16]).

Due to the different perspective, the detector percibes a fringe pattern with deformations that correspond to the object's contour as may be seen in Figure 1.3). These fringes are percieved at a different lateral position in accordance to the height of the surface, one could say the fringe follows the continuity of the surface shifting in accordance to changes in height. The height is thereby determined by means of the detected and reference position.

To appreciate these deformations, two different configurations may be used; crossed optical axis and parallel optical axis. Being the first one more common and the only one described in this chapter[1].

When using a crossed optical axis, the image is usually captured with the camera and projector at an angle β relative to the object as illustrated on Figure 1.4. When the angle is $90\,^{\circ}$, maximum sensitivity is achieved, however most of the shape is lost due to shadows. Since this angle is limited to peaks and valleys of the measured surface and a large angle may imply casting shadows over other areas of the surface. This angle may be understood by supposing that we are illuminating the surface laterally, just like the setting sun.

However, when the angle is $0\,^{\circ}$, it is not possible to appreciate these deformations. Therefore an angle no greater than the greatest slope in the object being measured is recommended [17] [18], trying to obtain the necessary sensitivity with the least possible information loss. Double detectors at $\pm\beta$ are often used to minimize these loses to shadows [19].

The shape is obtained from phase deviations on the image or images of the projected fringe pattern (deviations with respect to a reference, usually what the observer would appreciate if the fringe pattern impinged on a plane instead of the object) using sines and cosines that have the same period as the fringes on the captured image (pixels/period)[2]. The phase may be extracted by means of a trigonometric method, a transform or another process and an arctangent function that's generally valid in the $\pm\pi$ (or $\pm 180\,^{\circ}$) range. Figure 1.5 shows and example of the phase obtained from projecting fringes onto a baseball.

This information is wrapped in modulus 2π due to the cyclic nature of the sine and cosine. Therefore when a phase value is greater than π it will jump to $-\pi$ instead of increasing, and viceversa; as can be seen in Figure 1.6. So an unwrapping technique is usually used to remove discontinuities in the measurement.

Unwrapping consists in searching for the discontinuities and adding $\pm 2\pi$ to the rest of the phase map (under the consideration that there was a value greater than $\pm\pi$) obtaining continuous values as shown in Figure 1.7.

However, this is not valid when values equal or greater than $\pm 2\pi$ appear, and although in some cases it is possible to solve these indeterminations, this is an important consideration in carrier selection (a period large enough to avoid indetermination, but narrow enough to obtain enough information of the surface; this also must be physically realizable and capturable).

[1] Both are described in detail in the next chapter. Observations regarding the crossed axis configuration are also expanded upon, and properly demonstrated.

[2] Other types of functions such as Wavelet, have been employed [20]; the fringe pattern may also be interpolated by a function such as a Zernike polynomial or a collection of functions such as splines [16]

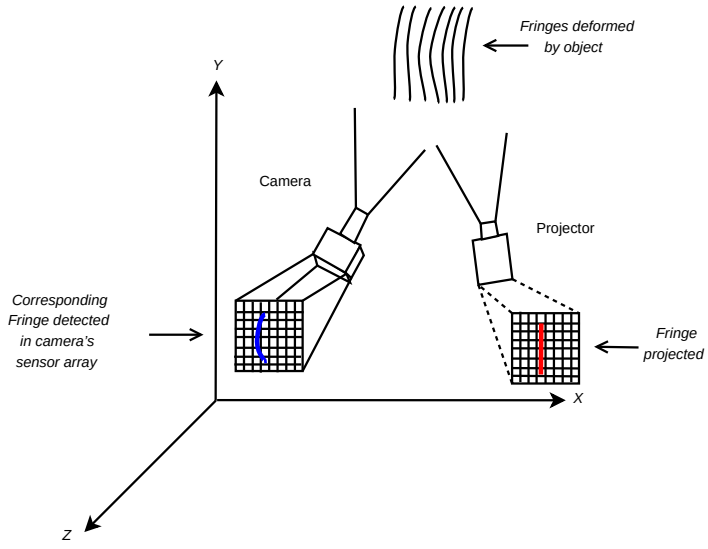

Figure 1.1: In this diagram the components of a fringe projection setup may be appreciated: the projector, detector and object. Fringes are deformed when impinging on the object. The red line shows a projected fringe, while the blue line shows the corresponding fringe deformed by the object that was captured by the detector.

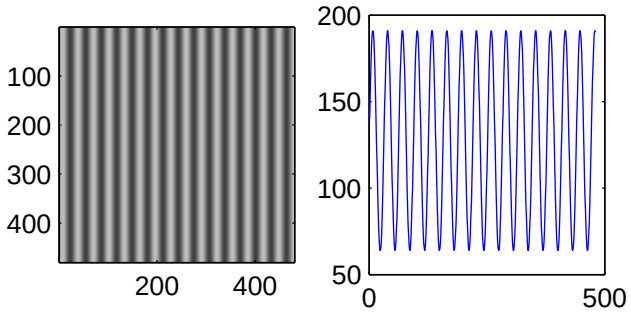

Figure 1.2: To the left, a sinusoidal fringe pattern; to the right, is a horizontal cut. One can appreciate the sinusoidal modulation of the intensity of light across the grid. The grid may have its fringes vertically, horizontally or at an angle.

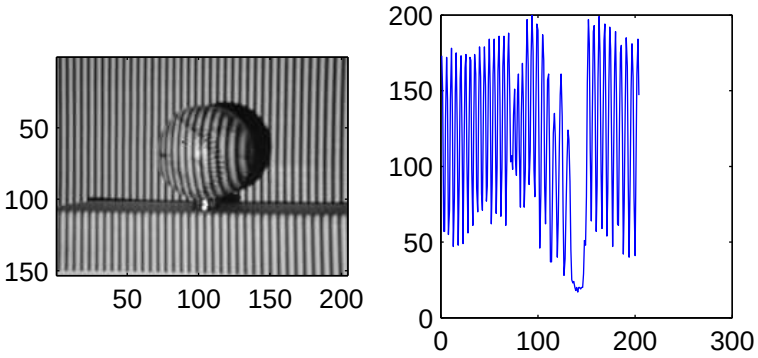

Figure 1.3: Left, an object with projected fringes; to the right, a horizontal cut of it's center. One can appreciate how the fringes deform to follow the baseball's contour.

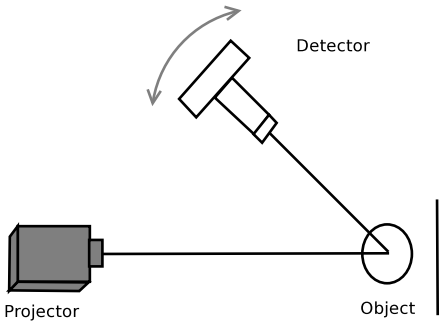

Figure 1.4: The camera and projector are at an angle β relative to the object. The greater the value of β the greater detail, at the cost of losing parts of the object to shadows.

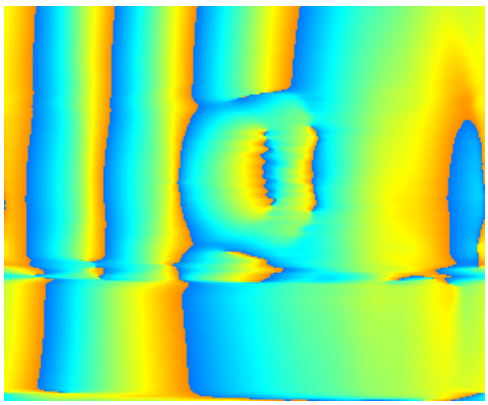

Figure 1.5: Phase distribution obtained from projected fringe pattern. Wrapping introduces discontinuities whenever the phase value exceeds the range of $\pm\pi$.

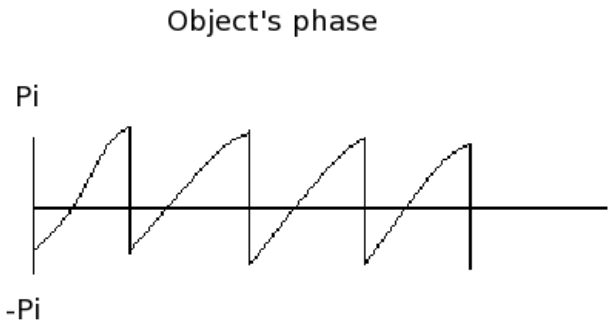

Figure 1.6: A diagram of a wrapped phase is shown. The discontinuities previously mentioned can be appreciated.

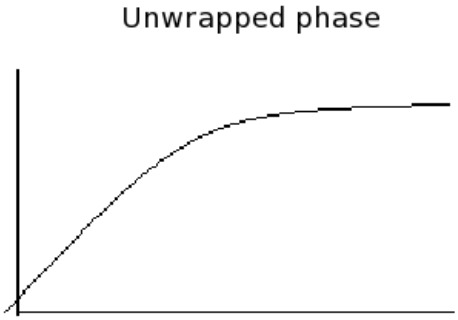

Figure 1.7: This diagram shows an unwrapped phase. One may appreciate continuity in the change of values.

Other relevant factors include phase values corresponding to shadowed parts of the object and noise present in practical applications.

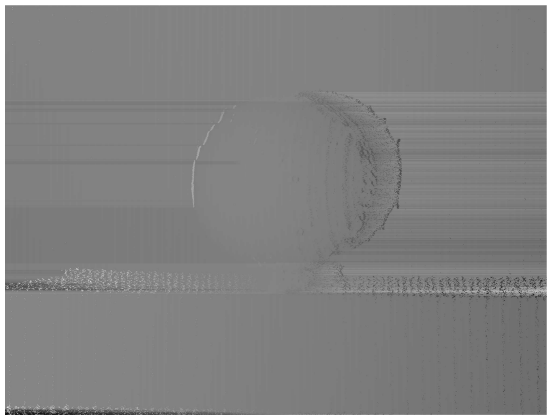

Figure 1.8: The unwrapped phase distribution corresponding to the same object is shown.

1.1.2 Interferometry

Interferometry is a set of techniques used to study the interference of waves. Optical interferometry being the most common and only studied in this thesis. Interferometic techniques have a lot of applications, including the fabrication of optical components, control and laser source manipulation, inspection and measurement of semiconductor waffles during VLSI manufacture [21]- [22] [3]- [23].

Two beam coherent light interferometers are very common. A ray passes through a beam splitter and both resulting rays go through a different optical path [24]- [16]. Then they are made to interfere generating a fringe pattern called interferogram, that contains the wavefront's intensity values. From this interferogram, information about the optical path difference may be obtained. Two common interferometer setups are the Twiman-Green and Fizeau interfereometers, who have a complementary nature.

1.2 Phase extraction

There are many algorithms and methods for phase detection (some use transforms, others correlation , other phase shifting, etc.) [16]- [24]. In this thesis we explore Carre's Asynchronous Algorithm. This is a phase shifting asynchronous algorithm that uses 4 samples to determine a phase value [14].

Phase shifting algorithms use a set of samples of a sinusoid that have a determined phase shift. When the algorithm needs a predetermined phase shift, it is called a synchronous algorithm. When this phase shift only needs to be the same between samples, the algorithm is asynchronous.

Samples may come from one or a set of pictures; in this work, we use single image analysis. This type of analysis is called asynchronous, since all samples are taken at the same time and the shift is called spatial since it is done within the space of the image [16].

1.3 Experiments and results

Carré's asynchronous algorithm is implemented using two different sampling criteria and is subjected to a set of numerical and physical experiments. Results of this algorithm are compared with the Diagonal Least Squares algorithm (a synchronous algorithm), Takeda's method (uses Fourier analysis) and Womack's Quadrature Multiplicative Moiré method [14]- [24]- [25].

In order to make these results useful, reliable and repeatable evaluation criteria are needed. So standard surface error measurement criteria were adopted [12], the error being defined by the reference minus the detected surfaces. Measurement criteria re divided into three groups, according to the surface error information provided: amplitude, spatial and hybrid. Amplitude criteria provide us with knowledge of the error's peak or average amplitude. Spatial parameter's indicate the regularity of this surface. And finally, hybrid criteria provide us with information about the magnitude of error variations.

These experiments were designed to represent characteristics common in measured surfaces. Five categories of experiments were chosen: Experiments based on an unmodulated carrier, step modulation, ramp modulation, quadratic modulation and spherical

modulation. Findings are described at the end of each experiment and then each each modulating wave form is discussed.

1.4 Conclusions

In the last chapter a global evaluation of the algorithm's behaviour on the basis of these results is given. Discussing findings and possible future research.

Bibliography

[1] D. Brune, R. Hellborg, H.J. Withlow, and O. Hunderi. *Surface Characterization: A user's sourcebook*. Wiley-VCH, 1997.

[2] Windecker Robert, Franz Stefan, and Tiziani Hans J. High-speed optical 3-d roughness measurements. *Proc. of SPIE*, 3824:105–114, 1999.

[3] D J Whitehouse. Surface metrology. *Meas. Sci. Technol.*, 9(8):955–972, 1997.

[4] Gottfied Frankowski, Mai Chen, and Tosten Huth. Optical measurement of the 3d-coordinates and the combustion chamber volume of engine cylinder heads. *Proc. of Fringe*, pages 593–598, 2001.

[5] Daniel Malacara. *Optical Shop Testing*. Wiley, 1992.

[6] Manuel Servin and Francisco Cuevas. A novel technique for spatial phaseshifting interferometry. *Journal of Modern Optics*, 42(9):1853–1862, January 1995.

[7] Gottfied Frankowski, Mai Chen, and Tosten Huth. Real-time 3d shape measurement with digital stripe projection by texas instruments micromirror devices dmd^{TM}. *Proc. of SPIE*, 3958:90–106, 2000.

[8] Quintana Xavier. *Modelling Stereoscopic Vision Systems for Robotic Applications*. PhD thesis, Universidad de Girona, July 2003.

[9] Song Zhang. *High Resolution, Real-time 3-D Shape Measurement*. PhD thesis, Stony Brook University, 2005.

[10] T. Peng and S.K. Gupta. Model and algorithms for point cloud construction using digital projection patterns. *ASME Journal of Computing and Information Science in Engineering*, 4(7):372–381, 2007.

[11] John G. Webster. *Instrument,Instrumentation and Sensors Handbook*. CRC PRESS, 1999.

[12] David J. Whitehouse. *Handbook of Surface Metrology*. CRC Press, 1994.

[13] Ayman Mohammad Samara. *Enhanced Dynamic Range Fringe Projection for Micro-Structure Characterization*. PhD thesis, University of North Carolina at Charlotte, 2005.

[14] Santiago Royo Royo. *Topographic measurements of non-rotationally symmetrical concave surfaces using Ronchi deflectometry*. PhD thesis, Universidad Politécnica de Catalunya, July 1999.

[15] Muhd Ibnur Rashad B. Zainal A., Gerald Liew Ming Jie, Mark Wee, Theresa Lai, Y. Fu, and H. M. Shang. A simple laboratory set-up for the fringe-projection method. (44588):316–319, 2002.

[16] Daniel Malacara, Servín Zacararias, and Cuevas Manuel. *Interferogram Analysis for Optical Shop Testing*. Marcel Dekker, Inc., 1998.

[17] Mitsuo Takeda and Mutoh Kazuhiro. Fourier transform profilometry for the automatic measurement of 3d object shapes. *Applied Optics*, 22(24):3977–3982, December 1983.

[18] Luis Salas, Esteban Luna, and Victor García. Profilometry by fringe projection. *Optical Engineering*, 42(11):3307–3314, November 2003.

[19] Quality control and 3d-digitizing using photogrammetry and fringe proyection, 2007.

[20] P. Tomassini, A. Giulietti, and L.A. Gizzi. Analyzing laser-plasma interferograms with a continuous wavelet transform ridge extraction technique: the method. Intense Laser Irradiation Laboratory - IFAM CNR, Pisa (Italy); The Queen's University, Belfast (UK); Blackett Laboratory and Imperial College, London (UK), February 2008.

[21] Deepti Tulsiani. A fringe projection system measurement of condensing fluid films in reduced gravity. Master's thesis, Worcester Polytechnic institute, 2005.

[22] Chris J. Evans Robert E. Parks Tony L. Schmitz, Angela Davies. Silicon wafer thickness variation measurements using infrared interferometry.

[23] Robert de Bruijn. *Heat Transfer in a Critical Fluid under Microgravity Conditions - a Spacelab Experiment -*. PhD thesis, Universiteit van Amsterdam, 1999.

[24] Johannes Schwider. Advanced evaluation techniques in interferometry. *Progress in Optics*, 28(22):271–359, 1990.

[25] Mitsuo Takeda, Hideki Ina, and Seiji Kobayashi. Fourier transform method of fringepattern analysis for computerbased topography and interferometry. *Optical Society of America*, 75(1):156–160, January 1982.